

Design of Wireless Energy Transmission Trackable Electric Car

Gang Zhao

North China University of Technology, Beijing 100000, China.

* Corresponding Email:13521415564@163.com

Abstract

With the development of wireless energy transmission technology, this topic takes MCU controller as the core, combined with PI algorithm, to design an intelligent electric car with wireless charging and automatic tracking. The system adopts a magnetic coupling resonant WPT, which supplies power to the supercapacitor bank through uncontrolled rectification boost and bidirectional Buck/Boost circuit. The Farad capacitor sends the power to the DC motor with a small driving current, and uses an infrared tracking sensing module to collect signals and transmit them to the MCU. The PWM pulse is adjusted in real-time to achieve automatic tracking of the electric car. Through testing, constant power wireless charging control and real-time driving of the car have been achieved, which can meet all requirements.

Keywords

Magnetic coupling resonant WPT; Supercapacitors; Infrared tracking; Intelligent control.

1. Scheme Demonstration and Comparison

1.1. Demonstration and Selection of Wireless Energy Transmission Schemes

Option 1: Magnetic induction coupled WPT

The principle is simple, easy to implement, with high transmission power and high efficiency in close range transmission. The working frequency ranges from tens to hundreds of kHz, with a relative transmission distance of several millimeters to several meters. But the magnetic flux leakage loss is large, the transmission distance is short, and the transmission efficiency decreases rapidly with the increase of transmission distance.

Option 2: Magnetic coupled resonant WPT

High efficiency, medium distance transmission, non radiative energy transmission, low electromagnetic radiation, and low electromagnetic interference outside the resonant frequency. The working frequency ranges from a few MHz to several tens of MHz, with a relative transmission distance of several centimeters to several meters^[3]. The transmitting and receiving coils need to have the same resonant frequency and high transmission efficiency, which are mainly used in electric vehicles and other fields.

Option 3: Microwave radiation type WPT

High precision directional energy transmission, with long transmission distance and relative transmission distance of hundreds to several kilometers. But the transmission efficiency is not high, the energy utilization efficiency is low, and the received power signal is small.

Option 4: Laser WPT

Good directionality, higher energy density, better convergence, and relative transmission distance of tens of meters to several kilometers. However, the transmission loss in the atmosphere is relatively large, requiring high accuracy and immature technology.

After comprehensive consideration, Scheme 2 is adopted: magnetic coupling resonant WPT.

1.2. Demonstration of Wireless Energy Transmission Transmitting Circuit Scheme

Option 1: Adopting a ZVS inverter circuit, without the need for external control signal driving, it can completely rely on its own to achieve oscillation, greatly improving the efficiency of the entire system. Due to the lack of external driving signal control, the self-excited oscillation circuit is unstable.

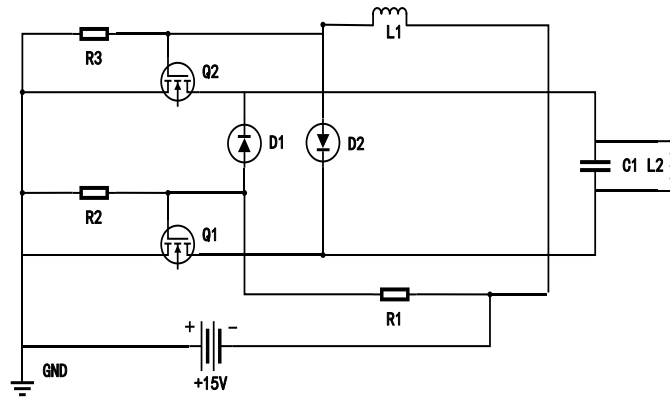


Figure 1 : ZVS Inverter Circuit

Option 2: Adopting a full bridge inverter and LCC series parallel resonant circuit, the full bridge inverter circuit has 4 bridge arms, with bridge arms 1 and 4 as a pair and bridge arms 2 and 3 as a pair. The two bridge arms in pairs conduct simultaneously, with each pair alternating 180° to generate a sine wave through LCC series parallel resonance.

According to the design requirements, the full bridge inverter and LCC series parallel resonant circuit can meet the design requirements and are relatively stable. After comprehensive consideration, Scheme 2 is chosen to design a wireless charging transmission circuit.

1.3. Demonstration of Wireless Energy Transmission Receiving Circuit Scheme

Option 1: Adopting LC parallel resonance and uncontrolled rectification filtering circuits, the efficiency of energy transmission is maximized when the transmission filtering, series parallel resonance of the circuit, and parallel resonance of the receiving circuit resonate simultaneously. After using diode uncontrolled rectification and filtering, the DC output is obtained through bidirectional Buck/Boost circuit transformation^[1].

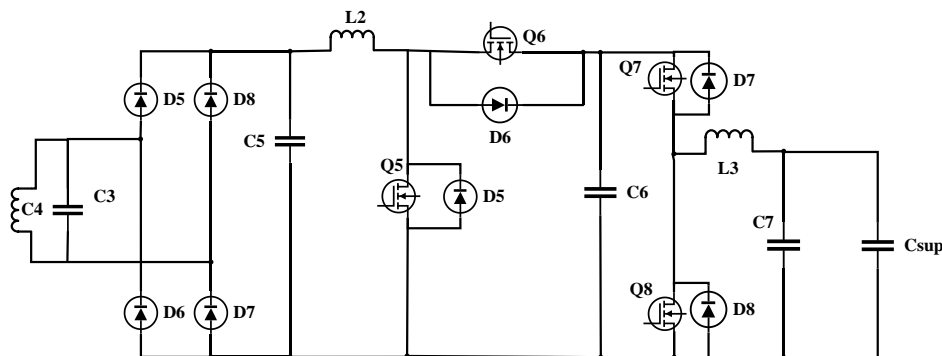


Figure 2 : LC Parallel Resonance and Uncontrolled Rectification Filter Circuit

Option 2: Use synchronous rectifier bridge rectification, as shown in Figure 3. Utilizing ideal bridge control chips such as LT4320 to control MOS transistors to achieve low voltage drop synchronous rectification, the conversion efficiency is extremely high.

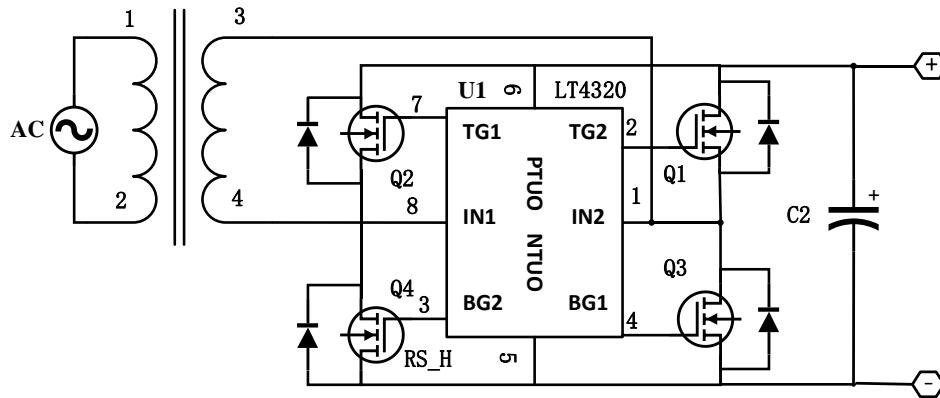


Figure 3 : Synchronous Rectifier Bridge Rectifier Circuit

Synchronous rectifier bridge rectification has higher conversion efficiency compared to uncontrolled rectification, but the circuit control is more complex and has current limitations. Therefore, a simple and stable uncontrolled rectification circuit is adopted, and Scheme 1 is chosen.

1.4. Demonstration and Selection of Automatic Tracking Scheme

Option 1: Photoelectric detector is adopted. When photoresistor detects the black line, the resistance value above the black line changes, and the comparison signal is sent to the microcontroller through the voltage comparator for processing, so as to control the automatic tracking of the car. But it is susceptible to the influence of external environmental light.

Option 2: Using infrared reflection detection, it has a pair of infrared emission and reception tubes. After the infrared is reflected, it is converted into electrical signals and sent to the microcontroller for processing, controlling the tracking of the car. Due to the use of infrared, it is not affected by external natural light and has a good tracking effect.

After the above analysis, the second option with strong anti-interference ability was selected.

1.5. Description of the Overall Plan

The entire solution has designed a wireless charging electric vehicle system that mainly includes a DC motor, supercapacitor, TCRT5000 infrared tracking sensor, driving circuit, and power supply. Among them, the microcontroller minimum system mainly realizes functions such as wireless energy transmission management, infrared tracking, and human-computer interaction. The wireless energy transmission system uses LCC series parallel resonance to transmit electrical energy, and LC parallel resonance to receive electrical energy. The system uses a bidirectional Buck/Boost converter to charge the supercapacitor, providing stable power supply for the control system and the car. The infrared tracking sensing module collects signals and transmits them to the MCU, and adjusts PWM pulses in real-time to achieve automatic tracking of the electric car.

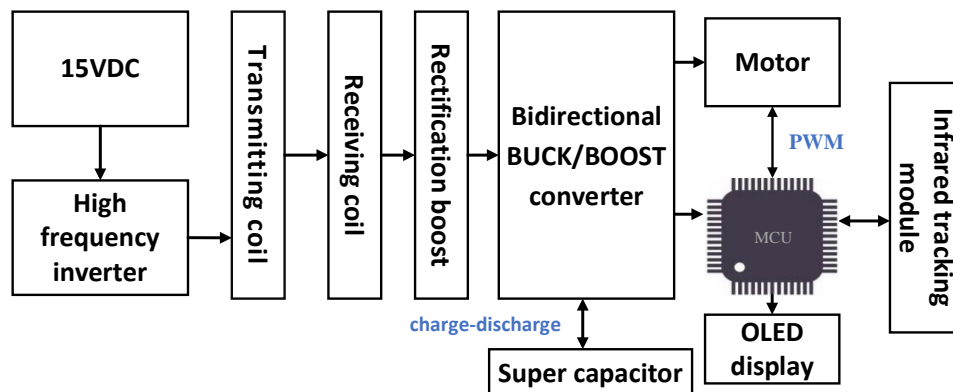


Figure 4 : Overall System Block Diagram

2. Theoretical Analysis and Calculation

2.1. Calculation of LCC Series Parallel Resonant Circuit

When resonant inductance L_1 and series resonant capacitor C_1 are working:

Resonance period $T_1 = 2\pi\sqrt{L_1C_1}$, resonant frequency $f_1 = 1/T_1$, resonant impedance $Z_1 = \sqrt{L_1/C_1}$;

When resonant inductance L_1 , series resonant capacitor C_1 , and parallel resonant capacitor C_2 are working:

The total capacitance of C_1 and C_2 in series is $C_{12} = C_1C_2/(C_1 + C_2)$, circuit impedance $Z_2 = \sqrt{L_1/C_{12}}$, resonance period $T_2 = 2\pi\sqrt{L_1C_{12}}$, resonant frequency $f_2 = 1/T_2$ [4].

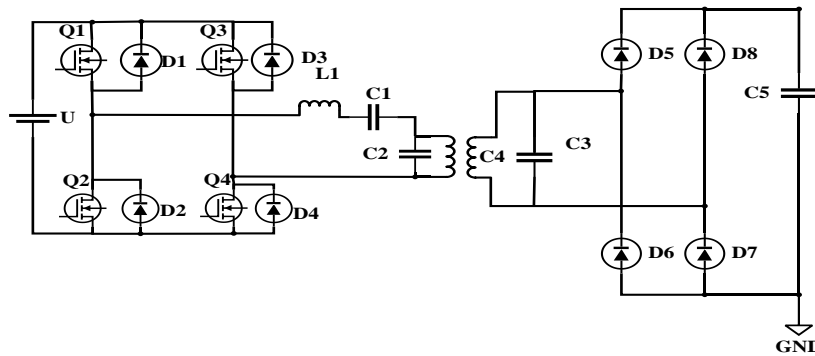


Figure 5 : LCC Series Parallel Resonant Main Circuit

After calculation, we obtained $L_1=28.67\mu\text{H}$, $C_2=353.3\text{nF}$, and $C_1=1\mu\text{F}$.

2.2. Calculation of Supercapacitor Selection Value

Reasonably select and design supercapacitors based on their charging characteristics. The energy released by capacitor discharge from the initial voltage U_1 to the threshold voltage U_2 during the operation of the car is [2]:

$$\Delta W = \frac{1}{2}CU_1^2 - \frac{1}{2}CU_2^2 \tag{1}$$

During this period, the capacitor output maintained a constant current I for t time, according to $Q=It$, obtained:

$$U(t) = U_1 - \frac{Q}{C} = U - \frac{It}{C} \tag{2}$$

By integrating the energy of the above equation, it can be obtained that:

$$C^2(U_1^2 - U_2^2) - 2UItC + I^2t^2 = 0 \tag{3}$$

To solve this equation, select the larger value as the reference value for selecting capacitance, then:

$$C = \frac{(U_1 + U_2)It}{U_1^2 + U_2^2} \tag{4}$$

According to the calculation, 8 capacitors with a capacity of 60F and a withstand voltage of 2.7V were selected as the supercapacitors. Through series connection, a capacitor bank with a withstand voltage of approximately 20V and a capacity of 7.5F was formed. When the charging voltage reaches 8V, it can store 240J of energy.

2.3. Simulink Simulation Verification

To ensure the feasibility of the system's main circuit topology, a wireless energy transmission model is built in the Simulink simulation environment to verify the feasibility of the model and

control strategy. By calculating and determining the LC resonance parameters, observe the voltage and current waveforms of the full bridge inverter, transmitting and receiving coils, and uncontrolled rectifier input.

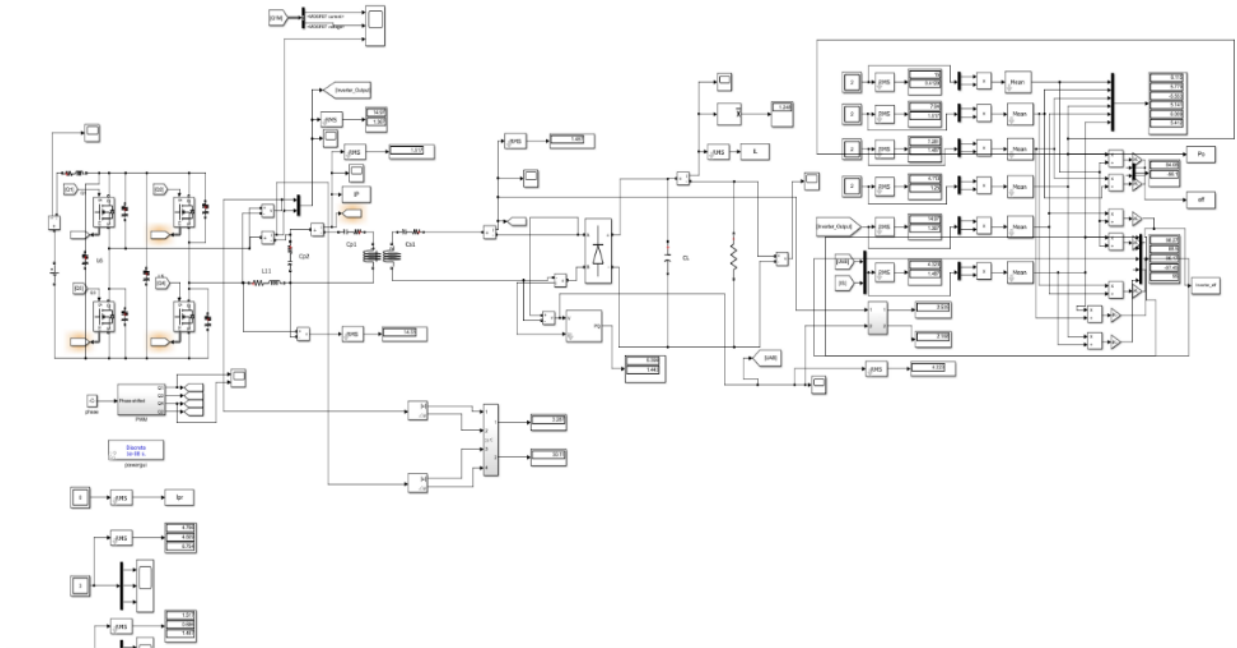


Figure 6 : Simulink simulation model

Through analysis and calculation, we obtained $L_{11} = 28.67\mu\text{H}$, $C_{p2} = 353.3\text{nF}$, $C_{p1} = 1\mu\text{F}$, and $C_{s1} = 689.26\text{nF}$.

The output voltage and current waveforms of the full bridge inverter, the current waveforms of the transmitting coil, the current waveforms of the receiving coil, and the input voltage waveforms of the uncontrolled rectifier bridge were observed, as shown in Figure 7.

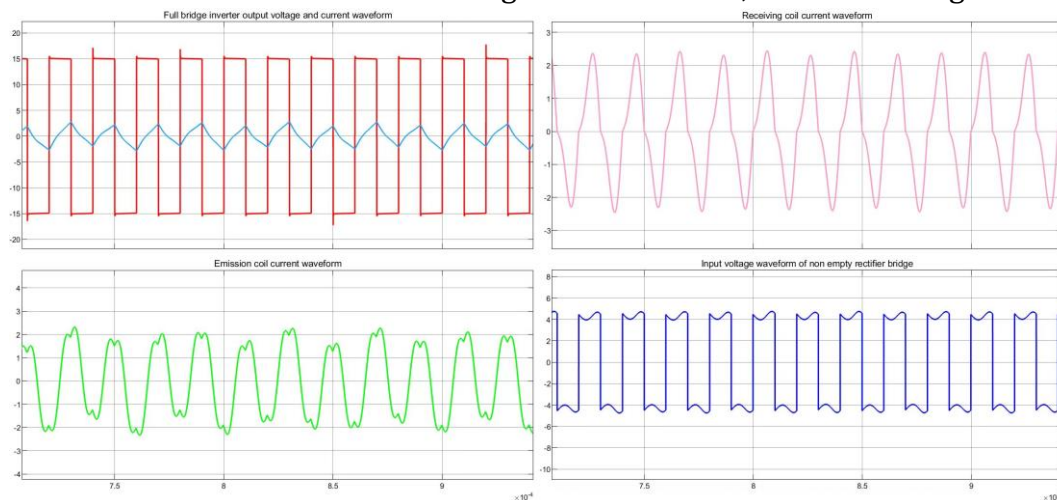


Figure 7 : Simulink simulation waveform diagram

The simulation results are consistent with theoretical analysis, and the output voltage of the rectifier bridge is 4.4V. At the same time, the correctness of the topology selection of the wireless charging main circuit was verified, and the theoretical analysis was consistent with the actual situation. The selected scheme was correct.

3. Circuit and Program Design

3.1. Design of the Main Circuit

The transmission circuit of wireless charging consists of a DC power supply, a high-frequency full bridge inverter, and LCC series parallel resonant circuit. 15V DC power is transmitted through high-frequency full bridge inverter and LCC series parallel resonance. The receiving circuit consists of LC parallel resonant circuit, an uncontrolled rectifier filter boost circuit, and a bidirectional Buck/Boost converter. When the series parallel resonance of the transmitting circuit and the parallel resonance circuit of the receiving circuit resonate simultaneously, the energy transmission efficiency reaches its maximum. After receiving AC power in the receiving coil, it is rectified and filtered to boost voltage, and converted into DC power to supply power to the supercapacitor bank. The main circuit topology of the system is shown in Figure 8.

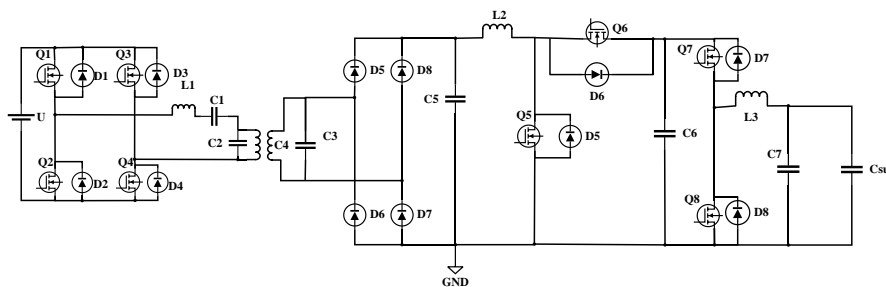


Figure 8 : System Main Circuit Topology

3.2. Overall Program Design

The software part includes the main function and timed interrupt function, which completes the microcontroller startup, system initialization, and human-machine interface display functions; The timed interrupt function is the main execution part of the software, completing vehicle charging, voltage detection, and infrared detection tracking.

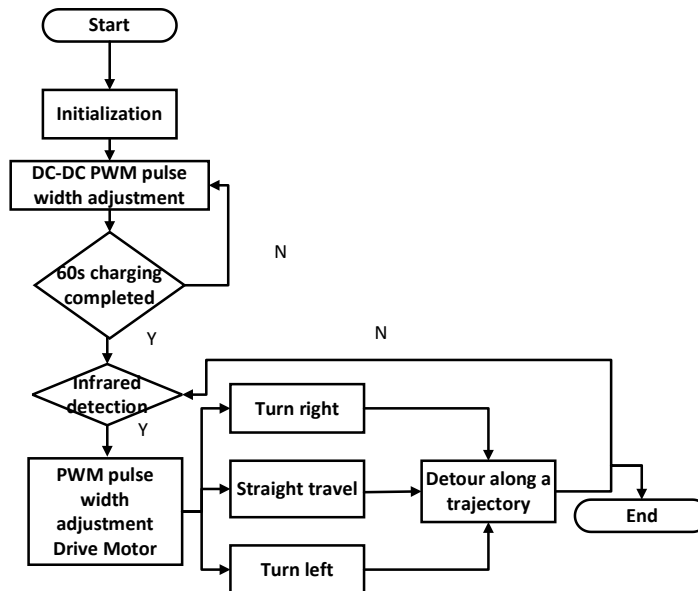


Figure 9 : Work flow diagram of electric trolley

3.3. Constant Power Software Design

The software control of charging power is based on the maximum constant power allowed for charging, and it is necessary to determine the maximum power during the charging process and control its power to ensure stability. Using PI closed-loop control and gradual probing methods, gradually reduce the voltage from no-load until the transmitter alarms to the maximum power

point, and ensure that the charging is controlled at that power. The flowchart of the constant power control program is as follows.

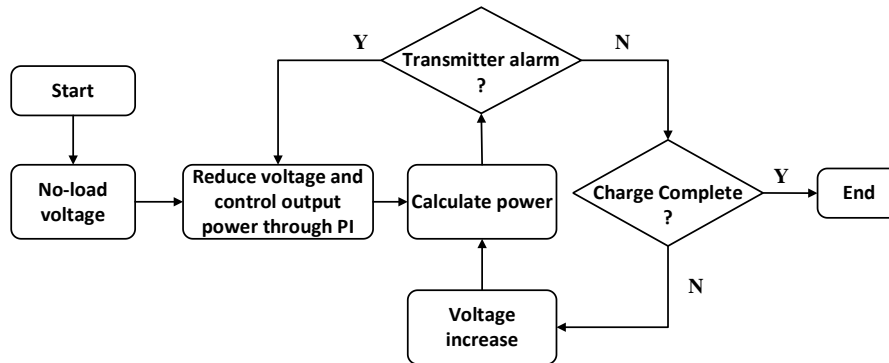


Figure 10 : Flow Chart of Constant Power Control Program

3.4. Design of Infrared Tracking Algorithm

To ensure the smoothness of the car's tracking process, a closed-loop PID control algorithm is adopted. The specific control model in this system is shown in Figure 10.

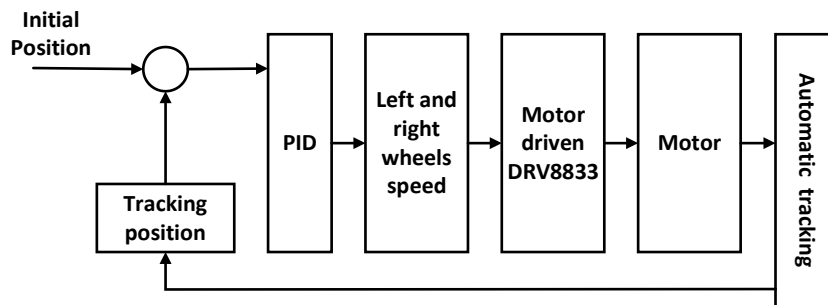


Figure 11 : PID Control System Flow Chart

There are two types of PID algorithms: positional and incremental. The output of positional PID is related to all past states and accumulates the errors each time, resulting in a large computational workload; Incremental PID is a recursive algorithm that subtracts the control amount at the current time from the control amount at the previous time, and uses the difference as the new control amount. Incremental PID control is adopted for the automatic tracking car system. The theoretical basis of the incremental PID control algorithm is:

$$u(t) = K_p(e(t) + \frac{1}{T} \int_0^t e(t) dt + T_D \frac{de(t)}{dt}) \tag{5}$$

After discretization:

$$u(k) = K_p(e(k) + \frac{T}{T_i} \sum_{i=0}^k e(i) + \frac{T_D}{T} (e(k) - e(k - 1))) \tag{6}$$

Subtraction of front and rear items:

$$\Delta u(k) = K_p \Delta e(k) + K_i e(k) + K_D (\Delta e(k) - \Delta e(k - 1)) \tag{7}$$

In the formula, K_p is the proportional control parameter; K_i is the integral control parameter; K_D is the differential control parameter.

In the actual software programming, the return value of the infrared sensor is taken as the error term. After PID calculation, the PWM duty ratio of the motor is changed, and the trolley steering is adjusted to automatically track.

4. Test Plan and Results

4.1. Test Content

(1) Use LED to indicate the power supply status of the car. When the car is powered, the LED will light up and there are no other energy storage and power supply devices on the car.

(2) The DC stabilized power supply powers the wireless charging transmitter for 1 minute and then turns off. The car immediately starts on its own and travels horizontally in a straight line until the energy is depleted. Record the distance traveled.

(3) After charging the electric car for 1 minute, drive along the black track on the ground and record the number of turns the car has traveled.

4.2. Test Result

Table 1 Test Content 1 Experimental Data

Number of experiments	Trolley power supply status	LED status
one	With electricity	bright
two	No electricity	Exterminate
three	With electricity	bright

Table 2 Test Content 2 Experimental Data

Number of experiments	Distance traveled by the car/m
one	eight
two	ten
three	nine

Table 3 Test Content 3 Experimental Data

Number of experiments	Number of driving laps of the car/lap
one	ten point one
two	ten point two
three	ten point one

4.3. Analysis of Test Results

Based on the above test data, the small car can effectively complete the first two basic requirements, and in the third basic requirement tracking, the small car can complete ten laps of driving. The car maintains good stability during operation. The physical image of the wireless energy transmission car is as follows.

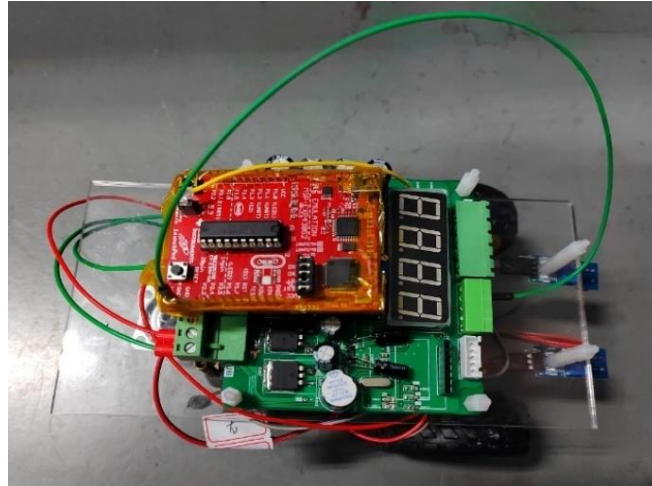


Figure 12 : Wireless Charging Trackable Electric Car

5. Summary

We have completed the design of a wireless charging trackable electric car, which can better meet the requirements of the question. And by comprehensively considering the design of the vehicle structure, reducing the vehicle weight and improving the charging and discharging efficiency, the driving distance of the electric car is increased.

References

- [1] Ma Xiaoshuang, Liang Hui, Ding Qing, Han Shilong. Research on Multiport Bidirectional Buck Boost Converter [J]. Power Electronics Technology, 2021,55 (05): 129-135.
- [2] Chen Xinyuan, Liu Yanfei, Li Hao, Wu Nana. Design of a constant power wireless charging intelligent balance car based on supercapacitors [J]. Electronic Components and Information Technology, 2021,5 (04): 45-47. DOI: 10.19772/j.cnki.2096-4455.20214.022.
- [3] Fan Xingming, Mo Xiaoyong, Zhang Xin. Research Status and Application of Radio Energy Transmission Technology [J]. Chinese Journal of Electrical Engineering, 2015,35 (10): 2584-2600. DOI: 10.13334/j.0258-8013. pcsee. 2015.10 twenty-six.
- [4] Liu Fucai, Jin Shuhui, Zhao Xiaojuan. Comparison of LC series resonance and LCC series parallel resonance in high-voltage pulse capacitor charging power supply [J]. High Voltage Technology, 2012,38 (12): 3347-3356.